NUMERICAL MODELING OF JET FLOW IN A SLOT CHANNEL IN THE TRANSITION REGIME

S. A. Safonov

UDF 532.546

Here we study the outflow of a viscous incompressible liquid from a rectangular nozzle into the submerged space of a Hele-Shaw cell (slot channel). The width of the nozzle is $d = 2r \gg h$, where h is the thickness of the cell. The configuration of the flow region is shown in Fig. 1. The characteristic linear dimension in the flow field is much larger than the thickness of the slot channel; therefore the change in the hydrodynamic characteristics of the flow in the horizontal direction can be determined by solving the two-dimensional equations of motion for quantities averaged in the vertical direction and by assuming that the vertical component of the velocity vector is zero.

Equations of motion have been obtained [1] in the two-dimensional approximation for a linear relationship for the friction with the cell wall. This relationship corresponds to the laminar region of Reynolds numbers $\mathrm{Re} = 2\bar{U}h/\nu$ ($\bar{U}$ is the average flow velocity in the slot channel). These equations of motion were used in a numerical analysis [1]. Laser Doppler measurements of velocity [1] in the plane of symmetry of the cell ($140 \leq \mathrm{Re} \leq 7000$) show that two regions form in the flow: a high-velocity jet flow dominated by inertial forces and a low-velocity jet flow. In the jet flow region, the streamlines are practically parallel to each other, and a sharp expansion of the jet occurs at its boundary. For $\mathrm{Re} > 3000$, the jet flow takes on a turbulent character and becomes laminar as it goes away from the opening of the nozzle and the axis of the jet. Friction at the cell walls is increased substantially in the turbulent regime, so a different friction relationship must be considered in the equations of motion.

Here we present a system of approximate two-dimensional equations which describe the jet flow in the slot channel in the transition regime (and which consider the laminarization of the flow). Results of a numerical analysis of these equations agree with experimental data [1].

The initial equations are the Reynolds equations, in which the vertical velocity component is assumed to be zero (the system of coordinates is chosen such that z = 0 is the plane of symmetry of the cell). The continuity equations are

$$u\partial u/\partial x + v\partial u/\partial y = -(1/\rho)\partial p/\partial x + \partial \tau_{xx}/\partial x + \partial \tau_{xy}/\partial y + \partial \tau_{xz}/\partial z,\ u\partial v/\partial x + v\partial v/\partial y = -(1/\rho)\partial p/\partial y + \partial \tau_{yx}/\partial x + \partial \tau_{yy}/\partial y + \partial \tau_{yz}/\partial z,\ \partial u/\partial x + \partial v/\partial y = 0. \tag{1}$$

If we integrate the system (1) along z from 0 to h/2, we obtain

$$\bar{u}\frac{\partial \bar{u}}{\partial x} + \bar{v}\frac{\partial \bar{u}}{\partial y} = -\frac{1}{\rho}\frac{\partial \bar{p}}{\partial x} + \frac{\partial \bar{\tau}_{xx}}{\partial x} + \frac{\partial \bar{\tau}_{xy}}{\partial y} + \frac{2}{h}\tau_{xz}|_{z=h/2} - D_x, \tag{2}$$

$$\bar{u}\frac{\partial \bar{v}}{\partial x} + \bar{v}\frac{\partial \bar{v}}{\partial y} = -\frac{1}{\rho}\frac{\partial \bar{p}}{\partial y} + \frac{\partial \bar{\tau}_{yx}}{\partial x} + \frac{\partial \bar{\tau}_{yy}}{\partial y} + \frac{2}{h}\tau_{yz}|_{z=h/2} - D_y,\quad \partial \bar{u}/\partial x + \partial \bar{v}/\partial y = 0,$$

where the bar above the quantities denotes averaging over the z coordinate; D_x and D_y are dispersion terms, which are related to the nonuniformity of the velocity profile in the direction of averaging (the problem of these terms is not modeled within the limits of this analysis).

In the laminar flow regime the viscous dissipation mechanism is not dominant, and the inertial terms in the equations of motion are basically balanced by the pressure gradient and by terms resulting from friction on the cell walls (excluding a narrow region next to

Novosibirsk. Translated from Prikladnaya Mekhanika i Tekhnicheskaya Fizika, No. 6, pp. 108-112, November-December, 1991. Original article submitted June 18, 1990.

0021-8944/91/3206-0920$12.50

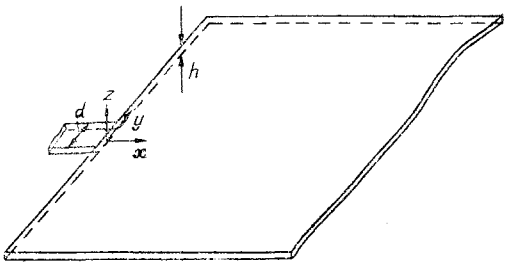

Fig. 1

the walls which are perpendiular to the plane of the cell). Also, in the turbulent regime, experiment [1] shows that the velocity profiles at the vertex have no flow perpendicular to the basic flow direction (as opposed to the corresponding profiles in the laminar regime). This indicates the importance of the turbulent flow mechanism and makes it necessary to model the turbulent transport terms in Eqs. (2), in order to have an adequate prediction of the hydrodynamic characteristics of the flow.

Because the transverse dimensions of the jet flow are much smaller than the longitudinal dimensions, we neglect derivatives of the tangential stresses with respect to x as compared to the derivatives with respect to y. We assume (ν_t is the turbulent viscosity).

We considered the following [two] representations for the turbulent viscosity: the Prandtl–Görtler viscosity $\nu_t = \delta\bar{u}(x, 0)$ for free turbulence ($\delta = c_t x$ is the width of the mixing zone and c_t is an empirical constant); and $\nu_t = \delta\bar{u}(x, y)$. In the second case it is assumed that $\nu_t \to 0$ near the boundary of the jet.

The velocity dependence of the friction at the cell walls is given as a sum of quadratic and linear functions, which correspond to the turbulent and laminar flow regions, respectively:

$$-\frac{2}{h}\tau_{xz}|_{z=h/2} = \frac{c_f}{h}\bar{u}V + 10\frac{\nu}{h^2}\bar{u}, \quad -\frac{2}{h}\tau_{yz}|_{z=h/2} = \tag{3}$$
$$= \frac{c_f}{h}\bar{v}V + 10\frac{\nu}{h^2}\bar{v} \qquad \left(V = \sqrt{\bar{u}^2 + \bar{v}^2}\right).$$

In dimensionless variables, the flow function $\bar{\psi}$ and the vorticity $\bar{\omega}$ of the system (2) have the form

$$\frac{\partial(\overline{u\omega})}{\partial x} + \frac{\partial(\overline{v\omega})}{\partial y} = \frac{\partial^2}{\partial y^2}\left(\left(10\frac{\mathrm{Da}}{\mathrm{Re}^*} + \nu_t\right)\frac{\partial\bar{u}}{\partial y}\right) + \tag{4}$$
$$+ \frac{\partial\Phi}{\partial y} + c_f\frac{r}{h}V^{-1}\left[(\bar{v}^2 - \bar{u}^2)\left(s\frac{\partial\bar{v}}{\partial x} + (1-s)\frac{\partial\bar{u}}{\partial y}\right) + 2\overline{uv}\frac{\partial\bar{u}}{\partial x}\right] -$$
$$- \bar{\omega}\left[c_f\frac{r}{h}\left(V + \frac{s\bar{u}^2 + (1-s)\bar{v}^2}{V}\right) + \frac{10}{\mathrm{Re}^*}\right],$$
$$\bar{\omega} = \Delta\bar{\psi}, \quad \Phi = \frac{\partial\nu_t}{\partial y}\frac{\partial\bar{v}}{\partial x} - \frac{\partial\bar{v}}{\partial y}\frac{\partial\nu_t}{\partial x}, \quad \bar{u} = \frac{\partial\bar{\psi}}{\partial y}, \quad \bar{v} = -\frac{\partial\bar{\psi}}{\partial x}, \quad s = \frac{1 + \mathrm{sgn}(\bar{u}^2 - \bar{v}^2)}{2}.$$

In Eqs. (4), the flow function is made dimensionless with respect to $\bar{U}r$, the vorticity with respect to $\bar{U}/r$, ν_t with $\bar{U}r$, and x and y with r. The reduced Reynolds number is $\mathrm{Re}^* = \bar{U}h^2/(r\nu)$, and the Darcy number for the Hele-Shaw cell is $h^2/(12r^2)$. Introducing the auxiliary function s in (4) makes it possible to avoid the instability in the iteration process of the numerical solution of this system of equations. For $c_f = 0$, the system (4) corresponds to Eq. (5) in [1].

The system (4) is solved by a finite-difference method. An "upwind" conservative difference method is used [3], which approximates the convective terms to first order. The resultant system of nonlinear algebraic equations is solved by the Gauss–Seidel iteration method. A nonuniform 76 × 41 grid is used with increased nodes near the corners of the nozzle opening. The dimensions of the calculational region in dimensionless variables were: width $\ell_y = 33$, length $\ell_x = 150$ (ℓ_y corresponded to the width of the slot channel in the experiments [1] and ℓ_x was chosen such that the boundary conditions at the right boundary did not affect the solution).

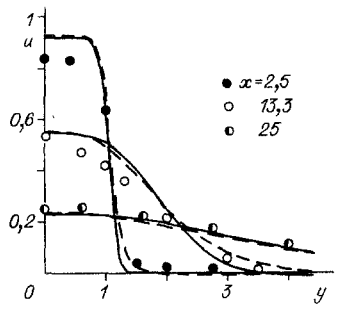

Fig. 2

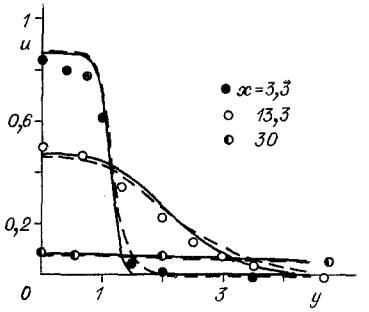

Fig. 3

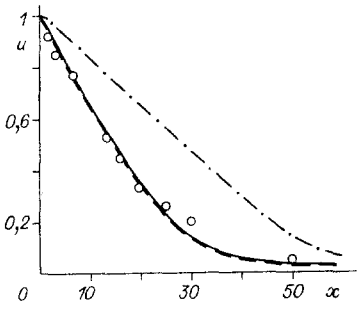

Fig. 4

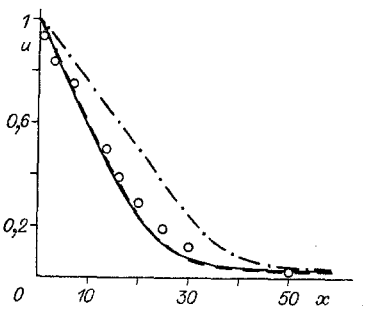

Fig. 5

The boundary conditions were as follows: at the solid boundaries of the flow field, $\bar{\psi} = 1$ and $\bar{\omega}$ was determined from the sticking condition described in Wood's form [3] to second order accuracy; on the axis of symmetry for $y = 0$, the flow was $\bar{\psi} = 0$ and $\bar{\omega} = 0$; on the right boundary ($x = \ell_x$) of the calculational region $\bar{\psi} = y/\ell_y$ and $\bar{\omega} = 0$ (that is, the fluid flow for $x = \ell_x$ is considered one-dimensional: $\bar{u} = 1/\ell_y$, $\bar{v} = 0$).

At the nozzle opening ($x = 0$ and $0 \leq y \leq 1$), the flow is assumed to be completely steady-state, that is $\partial\bar{u}/\partial x = 0$ and $\bar{v} = 0$. The profile of the longitudinal velocity component at the nozzle opening corresponds to the velocity profile for laminar flow, which is found by solving the equation

$$\mathrm{Da}(d^2\bar{u}/dy^2) - \bar{u} = \mathrm{const}, \tag{5}$$

which satisfies the conditions of constant mass flow and the boundary conditions

$$\int_0^1 \bar{u}\, dy = 1, \quad \frac{d\bar{u}}{dy}(0) = 0, \quad \bar{u}(1) = 0.$$

The velocity profiles at the nozzle opening, which correspond to turbulent and laminar flows, evidently differ insignificantly from each other for $d \gg h$, because, in the central part of the nozzle, they are close to constant along the y coordinate of the profile. Near the wall, the dissipative term in Eq. (5) is the basic effect on the velocity profile.

The numerical solution is considered to converge when

$$\max_{i,j} |1 - \bar{\psi}_{ij}^{(n+1)}/\bar{\psi}_{ij}^{(n)}| < 10^{-4}$$

where n is the number of iterations and $\bar{\psi}_{i,j}$ is the value of $\bar{\psi}$ at the node with coordinates i and j.

We note that the calculated velocities are determined as the average over the z coordinate in the slot channel, while the experimental velocity u_0 is measured in the plane of symmetry of the channel. The value of u_0 is made dimensionless with respect to the maximum velocity at the nozzle opening $u_0(0, 0)$: $u_0 = c\bar{u}/\bar{u}(0, 0)$, where $c = 1$ in the turbulent region and $c = 21/16$ in the laminar region, if we assume that the velocity profile is represented by a power law with an exponent of 1/7 in the turbulent region and by a parabola in the laminar region. As a result, the measured velocities, made dimensionless with respect to $u_0(0, 0)$, should exceed the calculated values by roughly 30% in the laminar region, that is on the periphery of the jet and at a sufficient distance "downwind" from the nozzle opening.

The calculated values of Re* = 370 and 525, and Da = 0.0036 corresponded to values in the experiment [1] (r/h = 4.8).

In the quadratic term of the friction equation (3), we chose $c_f = 0.0045$, which corresponds to the average value of c_f from Blasius' formula [4] for the transition region ($3{,}000 < Re < 10{,}000$); $c_t = 0.001$, which corresponds to c_t for the Prandtl–Görtler viscosity for the case of an axisymmetric jet [4].

Figures 2 and 3 show the calculated profiles of the longitudinal velocity component $\bar{u}/\bar{u}(0, 0)$ transverse to the jet for Re* = 525 for x = 2.5, 13.3, and 25 and Re* = 370 for x = 3.3, 13.3, and 30, respectively. The dashed curves correspond to the viscosity $\nu_{t1} = 0.001 \cdot x\bar{u}(x, 0)$ and the solid curves to $\nu_{t2} = 0.001 \cdot x\bar{u}(x, y)$. The points show the measured values of the ratio of the axial velocity [1] to the maximum value at the nozzle opening. The calculated curves, which correspond to these viscosities are in overall satisfactory agreement with the experimental results. Here the calculation with the viscosity ν_{t1} agree better with the test data near the jet axis and the calculations with ν_{t2} agree better at its periphery.

Figures 4 and 5 show the calculated curves for the axial velocity $\bar{u}/\bar{u}(0, 0)$ for Re* = 525 and 370 respectively (solid lines), and the points show the measured values $u_0/u_0(0, 0)$. The dash-dot lines, which correspond to the solution to the system (5) from [1] for a linear friction relationship, are much higher than the measured velocity values. The calculated curves for ν_{t1} and ν_{t2} practically coincide and reproduce the experimental data for $x < 15$ and Re* = 370 and for $x < 25$ and Re* = 525. At larger x values, the divergence between the measured and calculated values of the axial velocity in the plane of symmetry of the channel and the average [velocity] over its thickness is explained by the laminarization of the jet; in this case, as noted previously, the measured $u_0/u_0(0, 0)$ should exceed the calculated $\bar{u}/\bar{u}$ (0, 0) by roughly 30%.

Comparison of the calculated dependences and the experimental data shows that the modeling system (4) as a whole makes it possible to predict the development of jet flow in the slot channel in the transition regime.

LITERATURE CITED

1. V. D. Zhak, V. A. Mukhin, V. E. Nakoryakov, and S. A. Safonov, "Propagation of a submerged jet in a narrow slot," Zh. Prikl. Mekh. Tekh. Fiz., No. 3 (1985).
2. H. Görtler, "Calculation of the problem of free turbulence based on a new approximation," ZAMM, No. 22 (1942).
3. A. D. Gosmen, V. M. Pan, A. K. Ranchel, et al., Numerical Methods of Investigating the Flow of a Viscous Fluid [Russian translation], Mir, Moscow (1972).
4. H. Schlichting, Boundary Layer Theory [Russian translation], Nauka, Moscow (1974).